



A Multi-Node Thermal System Model for Lithium-Ion Battery Packs

Preprint

Ying Shi, Kandler Smith, Eric Wood,
and Ahmad Pesaran

*Presented at the 2015 American Control Conference
Chicago, Illinois
July 1–3, 2015*

**NREL is a national laboratory of the U.S. Department of Energy
Office of Energy Efficiency & Renewable Energy
Operated by the Alliance for Sustainable Energy, LLC**

This report is available at no cost from the National Renewable Energy Laboratory (NREL) at www.nrel.gov/publications.

Conference Paper
NREL/CP-5400-63898
September 2015

Contract No. DE-AC36-08GO28308

NOTICE

The submitted manuscript has been offered by an employee of the Alliance for Sustainable Energy, LLC (Alliance), a contractor of the US Government under Contract No. DE-AC36-08GO28308. Accordingly, the US Government and Alliance retain a nonexclusive royalty-free license to publish or reproduce the published form of this contribution, or allow others to do so, for US Government purposes.

This report was prepared as an account of work sponsored by an agency of the United States government. Neither the United States government nor any agency thereof, nor any of their employees, makes any warranty, express or implied, or assumes any legal liability or responsibility for the accuracy, completeness, or usefulness of any information, apparatus, product, or process disclosed, or represents that its use would not infringe privately owned rights. Reference herein to any specific commercial product, process, or service by trade name, trademark, manufacturer, or otherwise does not necessarily constitute or imply its endorsement, recommendation, or favoring by the United States government or any agency thereof. The views and opinions of authors expressed herein do not necessarily state or reflect those of the United States government or any agency thereof.

This report is available at no cost from the National Renewable Energy Laboratory (NREL) at www.nrel.gov/publications.

Available electronically at SciTech Connect <http://www.osti.gov/scitech>

Available for a processing fee to U.S. Department of Energy and its contractors, in paper, from:

U.S. Department of Energy
Office of Scientific and Technical Information
P.O. Box 62
Oak Ridge, TN 37831-0062
OSTI <http://www.osti.gov>
Phone: 865.576.8401
Fax: 865.576.5728
Email: reports@osti.gov

Available for sale to the public, in paper, from:

U.S. Department of Commerce
National Technical Information Service
5301 Shawnee Road
Alexandria, VA 22312
NTIS <http://www.ntis.gov>
Phone: 800.553.6847 or 703.605.6000
Fax: 703.605.6900
Email: orders@ntis.gov

Cover Photos by Dennis Schroeder: (left to right) NREL 26173, NREL 18302, NREL 19758, NREL 29642, NREL 19795.

NREL prints on paper that contains recycled content.

A Multi-Node Thermal System Model for Lithium-Ion Battery Packs

Ying Shi, Kandler Smith, Eric Wood, Ahmad Pesaran

Abstract— Temperature is one of the main factors that control the degradation in lithium ion batteries. Accurate knowledge and control of cell temperatures in a pack helps the battery management system to maximize cell utilization and ensure pack safety and service life. In a pack with arrays of cells, a cell's temperature is not only affected by its own thermal characteristics but also by its neighbors, the cooling system and pack configuration, which increase the noise level and the complexity of cell temperature prediction. This work proposes to model lithium-ion packs' thermal behavior using a multi-node thermal network model, which predicts the cell temperatures by zones. The model was parametrized and validated using commercial lithium-ion battery packs.

Index Terms— battery pack thermal management, lithium-ion battery, system modeling

I. INTRODUCTION

Hybrid electric vehicles (HEV) bring opportunities to reduce gasoline consumption and emission. Widespread electric vehicle adoption calls for more robust hybrid systems to work in different terrains and climates. This has brought more challenges to battery pack management and vehicle powertrain control. Among all the environmental variables, lithium-ion batteries' performance and service life are heavily affected by operating temperatures. Therefore, most lithium-ion battery performance models and battery life prognostic models are temperature-dependent. A battery pack's thermal performance is a result of the cell thermal properties, the cooling system configuration, and the pack packaging design. For vehicle system engineers, the detailed internal temperature map of a production pack is often not available due to non-disclosure agreements or the intellectual property of the pack manufacturers. Thus, vehicle system control engineers are often left to generate the thermal model of battery packs for macro-scale hybrid system controller design, implementation, simulation and testing based on only minimum, maximum, and average cell temperatures in the pack.

Computational fluid dynamics (CFD) models are popular tools for cell thermal behavior study and pack thermal management system design and analysis [1, 2, 3]. They have also been applied to safety simulation under abuse conditions [4]. Those models contain many details of the batteries and cooling paths to capture the internal temperature map of a lithium-ion cell or pack [5].

However, the nonlinearities, high dimensionality, and complex battery physics involved in CFD models all contribute to the high computation cost of such models. In addition, CFD models are closed systems which cannot be easily integrated with online controllers that requests real-time access of model internal states. Hence, large-scale hybrid powertrain controller design and simulation creates the need for high fidelity, low-order, computationally cheap and control-oriented system thermal models. A lumped thermal model is one suitable candidate [6, 7]. Such models have been applied to single cell systems [8] and battery modules [9]. Thermal network models were proposed to develop a low-order battery pack thermal model that can capture the heat transfer of a pack sitting in an HEV [10, 11, 12].

This work adopted the thermal network model idea to model large HEV and plug-in hybrid electric vehicle (PHEV) lithium-ion battery pack by partitioning battery packs into multiple zones and lumping each zone into a thermal node. Three-node and Four-node thermal models were proposed for commercial HEV and PHEV packs. The models were parameterized and validated with experimental pack thermal testing data.

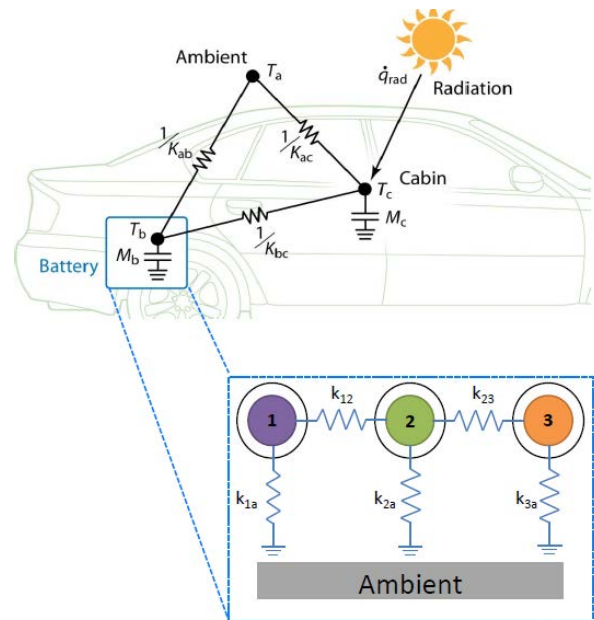


Figure 1. A schematic of the thermal network and the lumped thermal model

II. MODEL CONSTRUCTION

The temperature distribution in a battery pack is affected by its environment, radiation, cabin temperature, and ambient

*This work is supported by DOE Vehicle Technologies and ARPA-e AMPED Programs.

The authors are with the National Renewable Energy Laboratory, Golden, CO, USA 80401 (e-mail: ying.shi@nrel.gov; kandler.smith@nrel.gov; eric.wood@nrel.gov; ahmad.pesaran@nrel.gov).

temperature, as shown in Figure 1. The correlation can be modeled as a thermal network, with the battery pack represented as a lumped thermal mass and one temperature,

$$m_c \dot{T}_c = -k_{ac}(T_c - T_a) - k_{bc}(T_c - T_b) + \varepsilon A_c \dot{q}_{rad} \quad (1)$$

$$m_b \dot{T}_b = -k_{ab}(T_b - T_a) - k_{bc}(T_b - T_c) \quad (2)$$

or in the state-space form,

$$\begin{bmatrix} \dot{T}_c \\ \dot{T}_b \end{bmatrix} = \begin{bmatrix} -\frac{k_{ac} + k_{bc}}{m_c} & \frac{k_{bc}}{m_c} \\ \frac{k_{ab}}{m_b} & -\frac{k_{ab} + k_{bc}}{m_b} \end{bmatrix} \begin{bmatrix} T_c \\ T_b \end{bmatrix} + \begin{bmatrix} \frac{k_{ac}}{m_c} & \frac{\varepsilon A_c}{m_c} \\ \frac{k_{ab}}{m_b} & 0 \end{bmatrix} \begin{bmatrix} T_a \\ \dot{q}_{rad} \end{bmatrix} \quad (3)$$

However, in a battery pack with a long string of cells, instead of the overall average temperature, maximum and minimum cell temperatures are more of interests because they probably will grow into the worst and the least degraded cells, which define the boundaries of pack life estimates. To predict maximum and minimum cell temperatures, the battery pack can be partitioned into multiple zones. The cells in each zone should have little temperature variation; cells in different zone should have large temperature variation. Each zone can be presented with a lumped thermal mass (called a "node" in this work) and heat transfer coefficients. Zone division needs to be based on the pack design and thermal configuration. A straightforward division can have three zones, one containing the cells that have the most efficient cooling (most outside or upstream cells), one containing the cells that have the least efficient cooling (most inside or downstream cells), and one containing the rest of the cells in between. This three-node pack thermal model can be formulated as:

$$m_1 \dot{T}_1 = -K_{12}(T_1 - T_2) - k_{1a}(T_1 - T_a) + q_1 \quad (4)$$

$$m_2 \dot{T}_2 = -k_{12}(T_2 - T_1) - k_{23}(T_2 - T_3) - k_{2a}(T_2 - T_a) + q_2 \quad (5)$$

$$m_3 \dot{T}_3 = -k_{23}(T_3 - T_2) - k_{3a}(T_3 - T_a) + q_3 \quad (6)$$

where m_i and k_i represent the lumped thermal mass and heat transfer coefficients, respectively, of each zone, T_i indicate the zone temperature, and q_i is the heat generation in that zone. The state-space formation of the model is:

$$\begin{bmatrix} \dot{T}_1 \\ \dot{T}_2 \\ \dot{T}_3 \end{bmatrix} = - \begin{bmatrix} \frac{k_{12} + k_{1a}}{m_1} & -\frac{k_{12}}{m_1} & 0 \\ -\frac{k_{12}}{m_2} & \frac{k_{12} + k_{23} + k_{2a}}{m_2} & -\frac{k_{23}}{m_2} \\ 0 & -\frac{k_{23}}{m_3} & \frac{k_{23} + k_{3a}}{m_3} \end{bmatrix} \begin{bmatrix} T_1 \\ T_2 \\ T_3 \end{bmatrix} + \begin{bmatrix} \frac{1}{m_1} & 0 & 0 & \frac{k_{1a}}{m_1} \\ 0 & \frac{1}{m_2} & 0 & \frac{k_{2a}}{m_2} \\ 0 & 0 & \frac{1}{m_3} & \frac{k_{3a}}{m_3} \end{bmatrix} \begin{bmatrix} q_1 \\ q_2 \\ q_3 \\ T_a \end{bmatrix} \quad (7)$$

$$\begin{bmatrix} T_{max} \\ T_{min} \end{bmatrix} = \begin{bmatrix} \max(T_1, T_3) \\ \min(T_1, T_3) \end{bmatrix} \quad (8)$$

In this model, the only nonlinearity comes from the output equations.

If a pack is sitting in an isothermal environment, e.g. soaked in an environment chamber, the three-node pack model (described by Eq.7) will be sufficient. If in a vehicle and the pack is configured to use cabin air as the coolant, combining the pack model with the external thermal network (described by Eq.3) will be necessary. So the overall thermal model will be fourth-order with states $\{T_1, T_2, T_3, T_c\}$.

III. EXPERIMENT VALIDATION

The three-node pack thermal model was applied to two types of lithium-ion battery packs: HEV and PHEV packs. Thermal characterization tests were performed to regress the model.

A. Experiment Setup

Two HEV packs, from the same make but aged differently, were soaked solely in the chamber. One of the packs was wrapped with 2-inch thick insulation and fitted with the three-node pack thermal model. The PHEV pack was in a chamber with another pack and its convection and inlet air temperature were affected. Thus, it was fitted with a fourth-order pack thermal model with cabin temperature considered.

1) Thermal characterization test protocol

The thermal characterization test protocol consists of two parts: (1) step change of chamber (ambient) temperature, and (2) charge-sustaining (CS) cycles. The step test started by soaking the pack at 0°C, then setting the chamber temperature to 30°C for a day, and then returning the chamber set point back to 0°C. In the CS cycling, the pack was cycled under 10-second CS pulses at multiple C-rates, 0.5C, 1C, 1.5C, 2C, 2.5C, and 3C. During the CS cycling, the environment chamber was set to a fixed temperature of 30°C, 20°C, and 0°C.

From the test, the thermal capacitance and the heat transfer coefficients were identified for both packs. For CS cycling, heat generation rate was estimated from the data as

$$q_{total} = q_1 + q_2 + q_3 = I(V_{oc} - V)$$

where V_{oc} is estimated from a look-up table of $V_{oc} = f(SOC)$.

2) Pack thermal system setting

All the packs tested were cooled by forced air from the environmental chamber. The HEV packs had the fan on/off control as an inaccessible internal state. The fan turned on or off in the middle of CS cycling. Thus, all the CS cycling test results on HEV packs had both periods of fan on/off. The PHEV pack allowed the user to enable/disable cooling, but the fan was not turned on until control threshold was met. Separate CS cycling tests were conducted to run the pack with and without cooling.

B. Results and Discussion

1) HEV packs with three-node pack thermal model

The HEV packs were of the same make but had different aging histories. Nevertheless, the overall thermal mass of the

packs was expected to be the same and thus their thermal behaviors under step change tests should be very similar. Therefore, first, a single-node pack model was adopted to find the overall thermal mass of the packs using step change test data. The fixed pack total thermal mass was 42,100J/K. Second, in the three-node model, each node was assigned a portion of the total thermal mass. Based on the pack configuration, 10% was assigned to the two nodes representing the maximum and minimum and 80% was assigned to the node representing the rest of the cells. The models for each pack were regressed with both the step-change test and the CS cycling test to identify the thermal coefficients. Note that the pack thermal characteristics were much altered by the fan, so the model was independently fitted for the cases with and without cooling.

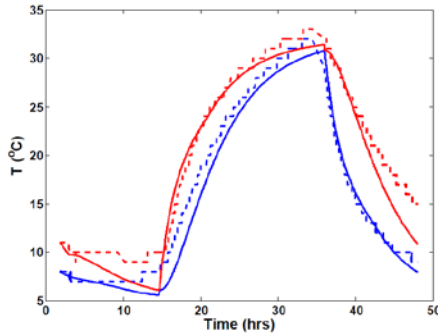


Figure 2. Ambient step change test of HEV pack 2: experiment data (dash) and model prediction (solid); max. cell temperature (red) and min. cell temperature (blue).

Figure 2 plots the experiment results of HEV Pack 1 and the pack thermal model prediction for the cell temperatures subject to step changes of the chamber temperature.

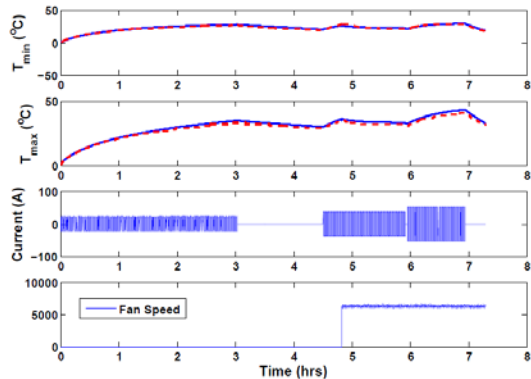


Figure 3. CS cycling test of HEV pack 1 at 0°C: experiment data (dashed lines) and model prediction (solid lines); maximum cell temperature (red) and minimum cell temperature (blue).

Figures 3 and 4 plot the experiment results and the model prediction of HEV Pack 1 subject to CS cycling tests at ambient temperatures of 20°C and 0°C. The top two subplots of each figure show the cell temperature measurements and prediction. The bottom two subplots are the corresponding C-rate and fan status. With the chamber set to 0°C, Pack 1 started at 1C and went through 1.5C and 2C CS cycles. The

fan was switched on shortly after the 1.5C CS cycling began and stayed on for the rest of the test. In the 20°C test, the pack underwent 0.5C, 1C, 1.5C, 2C, and 1.5C CS cycles. The C-rate was reduced because Pack 1 reached the maximum temperature. The cooling fan was switched on during 1C cycling and stayed on.

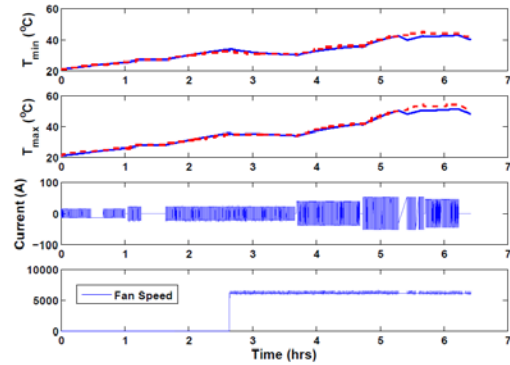


Figure 4. CS cycling test of HEV pack 1 at 20°C: experiment data (dashed lines) and model prediction (solid lines); maximum cell temperature (red) and minimum cell temperature (blue).

From the results, the three-node pack model of Pack 1 was able to capture the maximum and minimum cell temperatures. It followed the transient during step change and the temperature swings during CS cycling for most of the time.

Table 1
Fitted Thermal Coefficients for HEV Pack Thermal Models

Pack	Fan	T_a (°C)	k_{12} (w/K)	k_{1a} (w/K)	k_{23} (w/K)	k_{2a} (w/K)	k_{3a} (w/K)	RMS err (°C)
A	OFF	20	0.074	3e-11	4.2e-5	0.683	0.125	0.988
		0	0.081	0.124	0.089	0.94	0.274	1.176
	ON	20	5.1e-7	1.444	2.823	11.978	1.8e-6	1.884
		0	0.658	0.818	4.262	14.358	9.4e-8	1.208
B	OFF	20	9e-11	0.062	0.289	2.245	1e-14	1.884
		0	0.087	0.368	0.148	1.539	0.385	1.208
	ON	20	0.926	4.24	1.9e-6	13.896	1.789	1.773
		0	2.798	1.014	8e-5	31.249	1.975	1.709

The resolution of the pack temperature measurements was 1°C. The average root-mean-square (RMS) errors for the with-cooling and without-cooling cases are 1.1°C and 1.6°C, respectively. The model was only off by 2°C at 20°C after 5.3 hours. This was caused by the missing controller area network (CAN) data between 5.3 and 5.5 hours which made the model think the pack was at rest and cooled down, but the pack was actually not.

Figures 5, 6 and 7 show the experiment results and model prediction of HEV Pack 2 under step change and CS cycling. Pack 2 went through the similar CS cycling tests as Pack 1, only differing at the end of the 20°C test where the maximum cell temperature in Pack 2 was below the threshold and therefore allowed the test to go into the higher 2.5C-rate cycles.

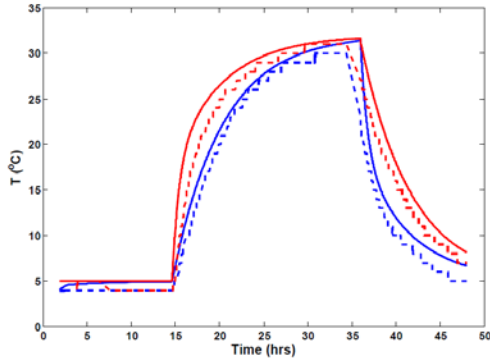


Figure 5. Ambient step change test of HEV pack 2: experiment data (dash) and model prediction (solid); max. cell temperature (red) and min. cell temperature (blue).

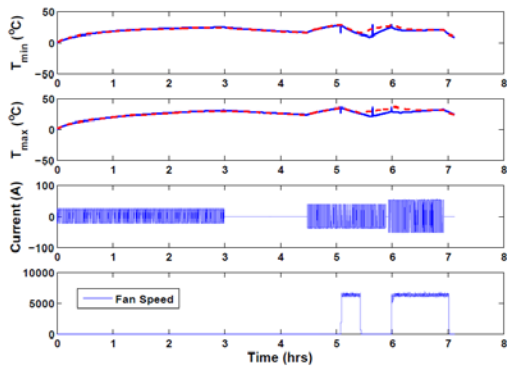


Figure 6. CS cycling test of HEV pack 2 at 0°C: experiment data (dashed lines) and model prediction (solid lines); maximum cell temperature (red) and minimum cell temperature (blue).

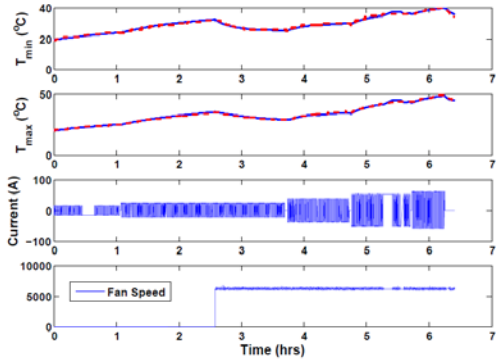


Figure 7. CS cycling test of HEV pack 2 at 20°C: experiment data (dashed lines) and model prediction (solid lines); maximum cell temperature (red) and minimum cell temperature (blue).

Pack 2's thermal model also captured the pack thermal performance well. With the fan on and off, the corresponding averaged RMS errors were 1.05°C and 1.5°C, respectively. The largest error occurred when the cooling fan turned off shortly during 1.5C cycling at 0°C. Table I lists all the fitted parameters and RMS error for the two HEV packs.

2) PHEV pack with fourth-order pack thermal model

A PHEV pack was characterized under the thermal test protocol described in Sec. III-A.1. A fourth-order pack thermal model with states $\{T_1, T_2, T_3, T_c\}$ was fitted to the data. The model was formed by plugging the states of Eq.7 into Eq.3. For this pack, a different fitting scheme was adopted. First, fix the assigned mass ratio of the three cell nodes, was set in this case, to be 12%, 76%, and 12%. Second, the thermal coefficient ratio of the three nodes was fixed, *i.e.*, $k_{1a} = c_1 * k_{ab}, k_{2a} = c_2 * k_{as}, k_{3a} = c_3 * k_{ab}$, and $\sum c_i = 1$. Similarly, the same c_i for $k_{i,c}$ and k_{bc} were used. Based on this pack's configuration, the ratios were estimated to be 0.24, 0.7, and 0.06. Then the experimental data were used to identify M_b, k_{ab} , and k_{bc} . Note that the average cell temperature plotted in the following figures was calculated by averaging measured maximum and minimum cell temperatures.

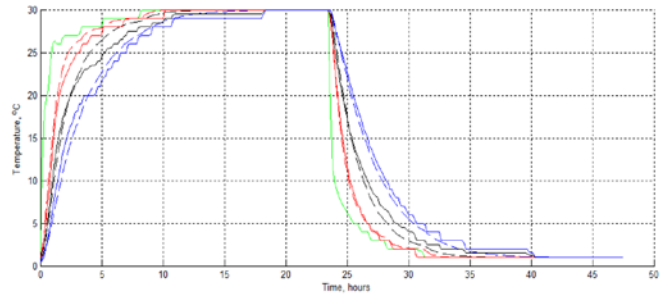


Figure 8. Ambient step change test of PHEV pack: experiment data (solid lines) and model prediction (dashed lines); maximum cell temperature (blue), average temperature (black), minimum cell temperature (red), and inlet air temperature (green).

Similar to the step change tests for HEV packs, the PHEV pack was soaked at 0°C, warmed up to 30°C for 24 hours, and then cooled down to 0°C for 24 hours. Figure 8 shows the measured cell temperature change along with step changes in chamber temperature.

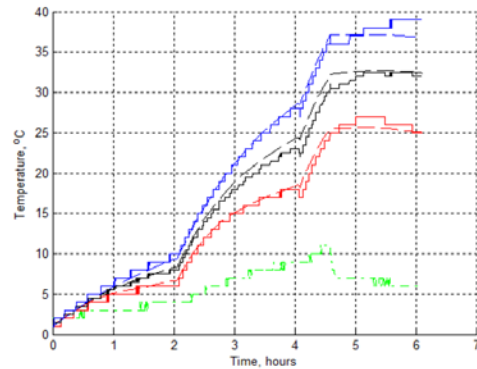


Figure 9. CS cycling test of PHEV pack at 0°C: experiment data (solid lines) and model prediction (dashed lines); maximum cell temperature (blue), average temperature (black), minimum cell temperature (red), and inlet air temperature (green).

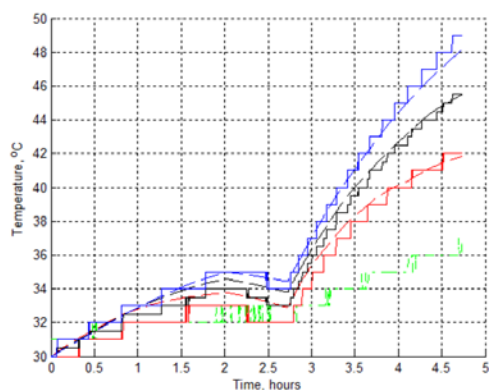


Figure 10. CS cycling test of PHEV pack at 30°C: experiment data (solid lines) and model prediction (dashed lines); max. cell temperature (blue), average temperature (black), min. cell temperature (red), and inlet air temperature (green).

The stair-like temperature curves were due to the 0.5°C resolution for the cell temperature measurements.

In CS cycling tests, the pack was cycled under 1C, 2C, and 3C currents at 0°C and 30°C. Figures 9 and 10 show the cell temperatures measured and predicted by the model. The model tracked the cell temperatures tightly at 0°C and 30°C.

Judging from the results, the fourth-order pack thermal model was able to capture the pack temperature change under step change and CS cycling. The fitted parameters for this pack are listed in Table II.

**Table II
Fitted Parameters for PHEV Pack**

$M_b(J/K)$	$K_{ab}(w/K)$	$k_{bc}(w/K)$
84,375	0.4	16

IV. CONCLUSION

This work modeled lithium-ion battery pack thermal performance using a thermal network with lumped thermal nodes. The resulting multi-node thermal model is low-order and can be explicitly described by ordinary differential equations. This makes it a convenient tool for vehicle system engineers to use in battery management system design. A three-node thermal model was fitted and validated for two HEV packs, focusing on pack thermal performance with directly heat exchange between a pack and the ambient temperature. The thermal masses in the models were fixed and the thermal coefficients were regressed from the experimental data. If considering heat exchange between a pack and the cabin, a fourth node representing the cabin can be added. Such a fourth-order thermal model was applied to a PHEV pack. The mass ratio and thermal coefficient ratio were fixed for the model. The overall pack thermal mass and the thermal coefficients with the cabin and the ambient temperature were identified using testing results. Both the three-node and four-node models successfully capture the maximum and minimum cell temperatures of the packs under step change tests and charge sustaining cycling. These models can be integrated with lithium-ion battery life model

or vehicle powertrain model for large-scale system simulation.

ACKNOWLEDGMENT

The initial thermal models for this work were developed by support from the Vehicle Technology Office, Office of Energy Efficiency and Renewable Energy, U.S. Department of Energy. Recent development for multimode development was supported by the DOE's Advanced Research Projects Agency-Energy, Advanced Management and Protection of Energy Storage Devices Program.

REFERENCES

- [1] A. Pesaran, S. Burch, and M. Keyser, "An approach for designing thermal management systems for electric and hybrid vehicle battery packs," presented at the Management Systems Conference and Exhibition, London, UK, May 1999.
- [2] T. Markel, A. Brooker, T. Hendricks, V. Johnson, K. Kelly, B. Kramer, M. O'Keefe, S. Sprik, and K. Wipke, "Advisor: a systems analysis tool for advanced vehicle modeling," *Journal of Power Sources*, vol. 110, no. 2, pp. 255 – 266, 2002.
- [3] N. Sato, "Thermal behavior analysis of lithium-ion batteries for electric and hybrid vehicles," *Journal of Power Sources*, vol. 99, no. 12, pp. 70 – 77, 2001.
- [4] K. Smith, G. H. Kim, E. Darcy, and A. Pesaran, "Thermal/electrical modeling for abuse-tolerant design of lithium ion modules," *International Journal of Energy Research*, vol. 34, no. 2, pp. 204–215, 2010.
- [5] G. H. Kim, A. Pesaran, and R. Spotnitz, "A three-dimensional thermal abuse model for lithium-ion cells," *Journal of Power Sources*, vol. 170, no. 2, pp. 476 – 489, 2007.
- [6] A. Pesaran, "Battery thermal models for hybrid vehicle simulations," *Journal of Power Sources*, vol. 110, no. 2, pp. 377 – 382, 2002.
- [7] V. H. Johnson, A. A. Pesaran, and T. Sack, "Temperature-dependent battery models for high-power lithium-ion batteries," presented at the 17th Annual Electric Vehicle Symposium, Montreal, Canada, October 2000.
- [8] C. Park and A. Jaura, "Dynamic thermal model of li-ion battery for predictive behavior in hybrid and fuel cell vehicles," *SAE Technical Paper*, 2003.
- [9] P. Nelson, D. Dees, K. Amine, and G. Henriksen, "Modeling thermal management of lithium-ion PNGV batteries," *Journal of Power Sources*, vol. 110, no. 2, pp. 349 – 356, 2002.
- [10] K. Smith, M. Earleywine, E. Wood, and J. N. et al., "Comparison of plug-in hybrid electric vehicle battery life across geographies and drive cycles," *SAE Technical Paper*, 01 2012.
- [11] K. Smith, A. Le, and L. Chaney, "National renewable energy laboratory strategic initiative working group report: Thermal model of gen 2 toyota prius," National Renewable Energy Laboratory," Technical Report, September 2009.
- [12] J. Neubauer and E. Wood, "Thru-life impacts of driver aggression, climate, cabin thermal management, and battery thermal management on battery electric vehicle utility," *Journal of Power Sources*, vol. 259, pp. 262 – 275, 2014